2012 6th Advanced Satellite Multimedia Systems Conference (ASMS) and 12th Signal Processing for Space Communications Workshop (SPSC)

Performance of a Combined Dynamic Rate Adaptation and Adaptive Coding Modulation Technique for a DVB-RCS2 System

Martina Angelone, Alberto Ginesi, Emiliano Re and Stefano Cioni
Communications and TT&C Systems and Techniques Section
ESA/ESTEC
Noordwijk, The Netherlands

***Abstract*—The growing demand for two-way broadband satellite services has pushed for the development of the DVB-RCS2 standard to improve the performance of the reverse link. Among the enhancements brought by the new standard, a wide range of modulation and coding schemes allows Interference and Fading Mitigation Techniques (IFMTs) to more efficiently exploit the diverse temporal and geographical propagation channel attenuations. In addition, the rich intra-system interference environment typical of large multi-spot beam network with high frequency re-use, and the constraints on the desired user QoS, call for a clever combination of different techniques. However, the effective implementation of the techniques is not trivial and the consequent benefits require the exploitation of complex computer-based system simulation tools. In this paper we compare the performance obtained for a DVB-RCS2 system using Adaptive Coding and Modulation (ACM) with those ones achieved by combining Dynamic Rate Adaptation (DRA) and ACM. The considered reference system is ka-band multi-spot beam network, which is deemed to follow within the next few years the current generation of ka-band HTS (High Throughput Satellites) networks.**

Keywords-DRA (Dynamic Rate Adaptation);ACM (Adaptive Coding and Modulation); DVB-RCS2; Interference and Fading Mitigation Techniques (IFMTs); return link

I. INTRODUCTION

In 2011, the DVB-RCS2 specifications [1] and [2] enhanced the flexibility allowed by the first generation of the standard ([3] and [4]) by adding additional waveforms and improving the overall performance of the return link. Indeed, besides the introduction of CPM (Continuous Phase Modulations), the new standard has increased the spectral efficiency range supported by the linear modulations through the introduction of 8PSK and 16 QAM schemes. In addition, a more powerful turbo code FEC scheme together with a quasi-constant length framing structure contribute to a more efficient exploitation of link adaptation techniques such as Adaptive Coding and Modulation (ACM) and Dynamic Rate Adaptation (DRA). In a system with ACM, each user selects the most efficient combination of modulation and coding (modcod) schemes allowed by the link on a burst-by-burst basis with the objective of maximizing the system throughput. The applicability of ACM in the reverse link of a multi-beam satellite broadband system has been already investigated in [5] and [6]. DRA is a technique which can be implemented by adopting carriers of different bandwidths in the system, so that each user can select the most appropriate carrier according to some criteria. In the past [7], [8] the performance achievable with DRA, ACM or their combination have been investigated and some strategies for applying jointly the techniques were proposed. In [7], the authors present performance analysis and numerical results related to the comparison of pure ACM with a pure DRA and a combination of DRA with variable coding. In [8], the authors compute an estimate of the efficiency of a pure ACM system using a set of modcods and they compare it with a DRA system where several symbol rates are available, but only one modcod is permitted. In addition, a combined ACM/DRA solution is investigated, where DRA is applied to cope with low probability severe fading events. In that approach, a small carrier is reserved for users undergoing extremely severe rain fading. This implementation of DRA is therefore aimed at improving the link availability whereas in nominal conditions only ACM is exploited. Whenever considering link adaptation techniques, it is worth to remark that an important issue in a DVB-RCS2 multi-beam system is related to the co-channel and adjacent channel interference variability. Indeed, in a MF-TDMA return link access, users sharing the same (or adjacent) carrier change on a burst-by-burst basis. As a consequence, the intra-system interference changes on a burst basis as well, thus it cannot be tracked due to the long closed loop delay of a Geostationary satellite link. Another important aspect that has been neglected in the literature so far, is the presence of the user terminal Out-Door Unit (ODU) operational point instabilities due to temperature, aging and control loop errors. This results in a statistical increase of the adjacent channel interference which might have detrimental effects particularly on the link availability.

In this paper we revisit the applicability of a combined DRA-ACM technique applied to a multi-beam system when taking into account all the aforementioned system imperfections and considering the newly standardized DVB-RCS2 waveforms. An assessment of the obtained performance is carried out by means of accurate system simulations and a comparison with the results of a pure ACM system is presented.

978-1-4673-2676-6/12/$31.00 ©2012 IEEE

The paper is organized as follows. Section II describes in detail the considered system model, the assumptions and the IFMTs algorithms. The interference calculation as well as the instability modeling are also described. In section III, the system requirement on the peak data rate is defined and its consequences on the calculated system parameters are presented. Section IV presents the simulation results and performance assessment of the considered scenarios. Finally, in section V conclusions are drawn.

II. SYSTEM MODEL AND ASSUMPTIONS

As previously stated, the object of this study is the return link of a multi-beam star transparent satellite access system based on DVB-RCS2. The considered scenario targets a network which can be considered the generation following the current HTS (High Throughput Satellite) systems like KaSAT and Viasat-1 and has been designed to fit possible evolutions of the current largest satellite platforms. The resulting system serves the users via a total of 200 user link beams, each allocated with 500 MHz in the Ka band in a 4 colors reuse pattern. The feeder link is assumed to operate in Q/V band in order to limit the required number of gateways. The considered system has therefore a very high frequency reuse factor of $f_R = 50$. In such context the impact of co-channel interference becomes indeed relevant.

The considered DRA-ACM system admits multiple symbol rates. The following assumptions have been done:

a) within each beam bandwidth, carrier segregation is applied (i.e. all the carriers with a given symbol rate and bandwidth are grouped together in sort of blocks over the frequency spectrum);

b) the organization of carriers within a beam is assumed to be repeated for all the user beams (consequently, co-channel carriers have the same bandwidth); with this hypothesis we assume coordination among the different gateways serving the full service coverage

c) the network is fully loaded and a perfect packet scheduler is considered, implying that all the bursts are filled;

d) both co-channel and adjacent channel interferers are always considered in clear sky, which is a worst case assumption although quite pertinent for both availability and capacity computations

e) Uniform traffic request is assumed

The reference propagation models are based on the most recent ITU recommendation [9].

In the following sub-sections, a detailed description of the adopted algorithms is provided.

A. ACM control loop

The advantages of adopting ACM on the return link of broadband satellite networks has been already shown in [5] and [6]. By changing the physical layer configuration based on the channel conditions, ACM optimizes the system efficiency and consequently its throughput. Considering UTs located in point (x, y) of a latitude-longitude coordinate system, we define the end-to-end instantaneous SNIR estimate as:

$$\frac{E_s}{(N_0 + I_0)}\left(x, y, T_{up}\%, T_{down}\%\right) \tag{1}$$

where $T_{up}\%$ and $T_{down}\%$ are the considered fading status on the user link and on the feeder link respectively. It is well known that ACM selects the modcod m whose required physical layer threshold fulfills the following conditions:

$$m \mid \begin{cases} \gamma_{req}(m) > \dfrac{E_s}{(N_0 + I_0)}\left(x, y, T_{up}\%, T_{down}\%\right) \\ \max\limits_{m}\{\eta(m)\} \end{cases} \tag{2}$$

where $\gamma_{req}(m)$ is the SNIR threshold associated to modcod m and $\eta(m)$ its spectral efficiency.

In the considered system, a set of 10 modcods are available for each UT. The related physical layer thresholds and efficiencies are listed in TABLE I.

Every link adaptation technique assumes the use of an adaptation loop. However, this loop is unable to track channel variations faster than the control loop delay, which is typically in the order of 1 second for a closed loop via geostationary transparent satellite. The ACM control loop for the considered reverse link has to deal with:

- the variation of rain fading within the loop delay;
- the SNIR estimation Root Mean Square Error (RMSE)
- the burst-by-burst SNIR variation due to the co-channel and adjacent channel interference

In order to take into account these elements, for the SNIR estimate it is assumed to have a negative envelop detector which detects the minimum instantaneous $E_s / (N_0 + I_0)$ as in [10].

TABLE I. CONSIDERED PHYSICAL LAYER

M	***Modulation***	***Code rate***	η^{a} ***[bit/symb]***	γ_{req} ***[dB]***
1	QPSK	1/3	0.607	0
2	QPSK	½	0.928	2.3
3	QPSK	2/3	1.304	3.9
4	QPSK	¾	1.472	5
5	QPSK	5/6	1.644	6.1
6	8PSK	2/3	1.754	8.2
7	8PSK	3/4	1.975	9.3
8	8PSK	5/6	2.195	11
9	16QAM	¾	2.662	11.6
10	16QAM	5/6	2.958	13

a. The efficiency includes pilots and guard symbols

B. Interference model and calculation

The UTs share the time and frequency resources according to conventional Multi-Frequency TDMA (MF-TDMA). As anticipated in the introduction, the traffic generated by UTs is bursty and its interference is therefore fast time varying: the position of the active interferer, either on the same carrier or on the adjacent carrier, varies burst-by-burst. In addition, the link condition of the considered user depends on the fading experienced during the burst.

In order to model the behavior of the negative envelope detector, within the system simulations, the ACM control loop is modeled by considering an interference power level that is exceeded with a probability lower than the target link packet error ratio. The rationale being that, assuming that an underestimation of the interference power level by the ACM control loop would cause a loss of a burst, the probability of this event has to be kept lower than the max allowed rate of packet losses.

This calculation is carried out considering at the same time co-channel and adjacent channel interference. At this regards, we recall assumption b). Assuming that in each beam, the UTs which use a certain symbol rate are located in the same frequency portion of the spectrum (segregation in carrier groups) it is possible to conclude that any interference comes only from users using the same symbol rate. This applies both co-channel and adjacent interference. In the latter case of course, the interferers belong to the same beam of the considered user. As the number of carriers within the beam is very high, all the users are considered interfered by two adjacent channel signals.

Recalling also assumption d), it is possible to conclude that the interference statistics are common to all the users of a beam using a certain symbol rate. This introduces the definition of class of interference. If the system admits N_{Rs} symbol rates (with $N_{Rs}=1$ in case of ACM) and has N_{beams} beams, the interference contribution which can be experienced by the users can be characterized as:

$$I(n,i) \quad n=1...N_{beams};\quad i=1...N_{Rs} \tag{3}$$

Note that the actual C/I depends on the instantaneous value of the considered user signal $C(x,y,T_{up}\%,T_{down}\%)$.

C. Combined DRA + ACM algorithm

In the considered system, a set of N_{Rs} nominal symbol rates are available. This implies that the UTs are able to support different carrier bandwidths. In the past literature, DRA has been sometimes used to increase the system availability by switching UTs experiencing high fading onto a very narrow symbol rate carrier with a given modcod. In these conditions, the link is closed by increasing the instantaneous SNIR due to the increased signal power spectral density, although with a penalized data rate.

In this analysis we propose an hybrid solution which uses DRA also in nominal conditions, i.e. clear sky, in combination with ACM. To this end, let us define the set of available symbol rates as:

$$Rs_i = \frac{Rs_{\max}}{2^{N_{Rs}-i}} \quad i=1...N_{Rs} \tag{6}$$

where $Rs_{\max}$ is the maximum symbol rate admitted by the system. In this case, the granularity of DRA is given, in dB, by:

$$Rs_{ratio_{dB}} = 10\log\left(\frac{Rs_{i+1}}{Rs_i}\right) = 3\ dB \tag{7}$$

In order to limit the impact of the adjacent channel interference, one approach is to use DRA to equalize the Power Spectral Density (PSD) of the received signals at satellite antenna input. In clear sky conditions in fact, assuming a constant symbol rate, the different users PSD levels are not equalized due to the satellite antenna gain geographical variation. The presence of fading also contributes to create power unbalance. Let us assume that $N_{Rs}=3$ and consequently $Rs_{\max}=Rs_{N_{Rs}}=Rs_3$. This means that if the power of a user is within 3 dB lower than the maximum power in the system, that user is assigned to Rs_3, if it is between 6 and 3 dB lower to Rs_2 etc…. Therefore, focusing on the user link of the considered system, a UT located in position (x,y) and experiencing a fading event with probability $T_{up}\%$ is assigned to the symbol rate *Rs* as follows:

$$Rs = \frac{Rs_{\max}}{(Rs_{ratio})^j} \tag{8}$$

where:

$$j = \left\lfloor \frac{C_{up}^{CS}\big|_{\max} - \left(C(x,y)\right)_{up}^{T_{up}\%}}{Rs_{ratio_{dB}}} \right\rfloor \tag{9}$$

where $C_{up}^{CS}\big|_{\max}$ is the maximum *signal power* (in [dB]) of the system in clear sky condition. Note that $T_{up}\%$ can refer also to clear sky. The described DRA procedure can be implemented at the network gateways where it is possible to estimate the user up-link SNR by measuring the end-to-end link SNR and subtracting off an estimate of the feeder down-link SNR (e.g. through a beacon or a composite processing of all the received carriers). Thus, the different UT PSDs are equalized within the DRA granularity both in clear sky and under fading condition, as long as the losses do not exceed the DRA dynamic range $\left[Rs_{ratio_{dB}} \cdot N_{Rs}\right]$. On top of DRA, i.e. after that the symbol rate has been assigned as above, ACM is applied as an outer control loop, by measuring at the GW the end-to-end instantaneous SNIR. The modcod is then selected in order to close the link with the most efficient waveform. In so doing, ACM is left to cope with limited SNIR variations. A high level functional diagram which describes the combined ACM and DRA scheme is given in Figure 1. For each UT, DRA is carried out first by

assigning the symbol rate in order to equalize the UT's power spectral densities. Once the symbol rate is known, the ACM control loop can estimate the current SNIR and select the most efficient modcod.

The clear advantages of applying this combined DRA+ACM solution is the following: the adjacent and co-channel interference contributions are reduced thanks to the signal PSD equalization at the satellite antenna input. Note that as far as the adjacent channel contribution is concerned, this reduction also applies to clear sky conditions (the antenna beam gain roll-off is equalized by the carrier group segregation), thus implying a possible capacity gain. In fading conditions, moving carriers under fading conditions to lower symbol rates is also expected to increase the system availability. Also, the DRA+ACM system implies an increase of complexity in the UTs and in the resource management and packet scheduling, which has to deal with different symbol rates and still has to efficiently use the available bandwidth.

D. Out-Door-Unit (ODU) Instabilities

As outlined in [4], two of the main components in an RCS user terminal (UT) are the Outdoor Unit (ODU) and the Indoor Unit (IDU). The ODU consists of a transceiver which includes a Solid State Power Amplifier (SSPA) with its driver, whose gain can be adjusted by a power control loop around the SSPA. The ODU can be affected by significant instabilities in terms of amplifier operating point (Output Back Off) due to temperature, aging and control loop measurement errors. These sources of instabilities result in different effects, both at the input (as IBO variations) and at the output (saturation power and SSPA characteristic instabilities) of the SSPA. Assuming statistical independence of these effects, one can assume to sum them up and consider their contribution as a Gaussian variable. In our system, this aspect is taken into account by modeling the SSPA Output-Back-off (OBO) as a Gaussian random variable in dB. The mean value of the distribution is the nominal OBO in dB of the optimum operation point and its standard deviation is $\sigma = 0.5$ dB. The obtained distribution has been truncated at OBO=0 dB.

This phenomenon has of course an impact in terms of adjacent channel isolation (ACI) and channel-to-inter-modulation ratio (C/IM). The first term is defined as the ratio between the in-band and the out-of-band power transmitted by a UT, while the C/IM takes into account the amount of distortion, i.e. inter-modulation products, generated by the SSPA. Indeed, depending on the modulation order and on the OBO used, each terminal is affected by a different C/IM and produces a different interference onto the adjacent carriers. In order to calculate these values for each terminal considered in our system, and for its related OBO, a Rapp Model with S=3 has been considered. The C/IM and ACI as a function of the IBO have been derived and the trend of considered look-up tables are shown in Figure 2 and Figure 3.

III. PEAK DATARATE REQUIREMENT

In the previous sections we described our system assumptions and the considered models. We want now to introduce the figures of merit and the system constraints with the objective of carrying out a fair comparison between pure ACM and combined ACM/DRA techniques.

The user data rate is impacted by both ACM and DRA in terms of selected modcod and symbol rate. A significant QoS parameter is represented by the peak data rate which can be offered to the users. A fair way to compare the two techniques is therefore to fix the minimum target peak data rate offered to the user R_{b_min}, and a percentage of the coverage where this data rate has to be guaranteed, for example $P_{\text{cov}}\% = 90\%$.

Another key figure of merit is of course represented by the system capacity, defined as the aggregated throughput that the system can offer. It can be shown that a trade-off between throughput and peak data rate exists: the higher the required user peak data rate (which imposes the network symbol rates), the lower the resulting aggregated system capacity. This is because the capacity per beam is proportional to the average spectral efficiency of the UTs, which reduces as the symbol rate increases. At this regard, we recall that

$$\left(\frac{C}{N}\right) = \left(\frac{C}{N_0}\right) \cdot \frac{1}{Rs} \tag{10}$$

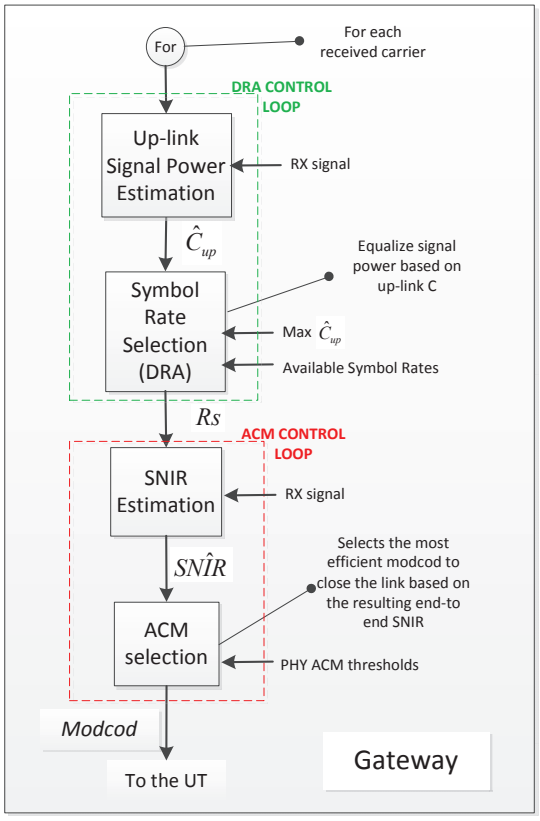

Figure 1 Combined ACM and DRA process functional diagram

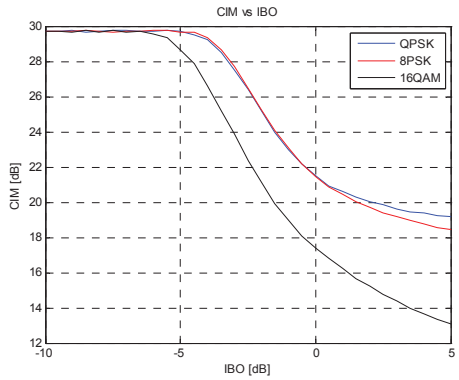

Figure 2 Considered SSPA C/IM as a function of the IBO for the each modulation used in the system

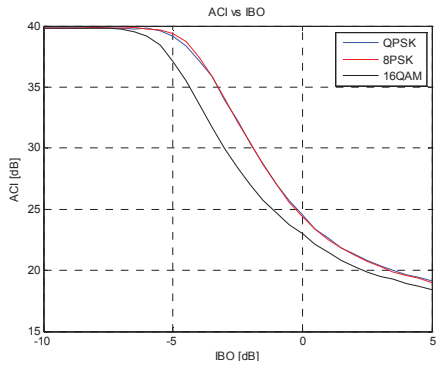

Figure 3 Considered SSPA ACI as a function of the IBO for the each modulation used in the system

Indeed, the trade-off between offered data rate and total throughput is not trivial. In addition, the probability of outage shall be taken into account. For each UT, we define this figure as the sum of the probabilities of the events which cause an outage.

IV. Simulations Results

In this section, the set of results obtained by means of end-to-end system simulations is reported. A performance comparison between a system employing pure ACM and one using the combined technique is presented. All the simulations have been carried out based on the assumptions a) to e).In TABLE II. the main link budget parameters are summarized, while satellite RX beam pattern and the position of the gateways is shown in Figure 4.

An exhaustive search of the symbol rate (or set of symbol rates) which guarantees the minimum target peak rate of 25 Msps over the 90% has been carried out by means of clear sky link budget analysis. The following symbol rates have to be adopted in the two cases:

- 16.7 Msps, in case of ACM only
- 8.4, 16.7 and 33.3 Msps in case of ACM+DRA

TABLE II. Link Budget Parameters

System Parameters				
Parameter	***Value***			***Unit***
Required Minimum Peak Rate	25			Mbps
Required Coverage Percentage	90			%
User Terminal Parameters				
Parameter	***Value***			***Unit***
SSPA Saturated Outpu Power	2			W
SSPA Nominal OBO	QPSK	8PSK	16QAM	dB
	0.5	0.75	2.5	
UT antenna diameter	60			cm
UT antenna efficiency	0.6			
UT TX lossess (output+pointing)	1			dB
Payload Parameters				
Satellite Antenna Peak RX Gain (user link)	57			dBi
Satellite G/T	27			dB
Repeater Noise Figure	3.5			dB
Satellite Antenna Peak TX Gain (feeder link)	54			dBi
Feeder Q band on-board TWTA Saturated Output Power[a]	100			W
Feeder Q band on-board TWTA OBO	6			dB
Feeder Q band on-board TWTA Output Loss	4			dB
Feeder Q band on-board TWTA NPR	23			dB
Gateway Parameters				
Gateway Antenna Diameter	4.5			m
Gateway Antenna Efficiency	0.65			
G/T	38			dB
LNA Noise Figure	2			dB
Total Losses	1.4			dB

a. Over 2 GHz bandwidth

The distribution of the DRA symbol rates over the coverage in clear sky is represented in Figure 5.

As already stated, the aim of DRA is to equalize the power spectral density of the useful signals at satellite level and consequently their C/N. The result of this equalization is shown in Figure 6, where it is clearly indicated that over the coverage the resulting up-link C/N range corresponds exactly to the selected DRA granularity (3 dB). An interesting comparison is represented indeed by the PDF of the adjacent C/I in clear sky. Based on the Montecarlo simulation and on the methodology described in Sect. II.B, the worst-case values of adjacent interference have been calculated. Thus, for each beam and for each symbol rate, the corresponding value of interference is known and the distribution of the C/I can be calculated per point based also on the clear sky useful signal power. The application of DRA and its consequent equalization, allows reducing sensibly the range of adjacent channel interference. This result is evident from Figure 7, where the minimum C/I obtained without using DRA is around 4 dB higher than in the other case. The large adjacent C/I dynamics when only ACM is used is caused by mainly two aspects: the first is the power spectral density unbalance between adjacent carriers belonging to UT's in different geographical positions (the antenna gain pattern may vary up to 4.5 dB within a beam); the second is the terminal's ODU power instabilities and thus out-of-band

emissions which randomly affects the interference between adjacent carriers.

The previous results are related to clear sky. As soon as fading events are taken into account another advantage of using DRA is evidenced: by increasing the ACM range, DRA increases also availability. In Figure 8 and Figure 9 the time-averaged distribution of up-link C/N and C/I respectively are compared for the two systems: in both cases, the statistics obtained applying also DRA (dashed line) show better values especially for low probability events (i.e. fading). For example, the average C/N value corresponding to a 10^-3 probability event is 5.5 dB with ACM only and 8.5 dB with ACM+DRA. Note that this difference corresponds exactly to the DRA granularity. For the C/I the advantages become more evident under heavy fading events. The consequent gain in availability is reflected also in Figure 10, where it is shown how the average outage probability varies over the coverage, in the two study cases.

For an end-to-end availability of 99.5%, only 35% of the coverage closes the link when using ACM only, while this figure increases up to 86.5% of the coverage in case the combined scheme is applied. On the other hand, it is interesting to remark that users which have a high SNIR in an ACM-only system are switched to a larger symbol rate when applying DRA: this mechanism, which is part of the equalization algorithm, limits the exploitation of the ACM range and of the highest efficiencies. An example of this effect is shown in Figure 11, where the use of DRA results in a more concentrated selection of modcod QPSK 5/6 compared to the ACM-only case, where the use of 8PSK or of the lower modcods is more frequent. Finally, TABLE III. summarizes the performance results related to the two study cases under investigation.

The two system gives very similar performance in terms of throughput. After all, the less spectral efficient access mechanism implied by the joint exploitation of ACM and DRA is compensated in terms of performance penalty by the reduction of adjacent interference power. This result is of course quite scenario-dependent but is still representative and shows that the use of DRA does not necessarily implies a reduction on spectral efficiency. In addition, a remarkable benefit of DRA is shown in Figure 12, where the peak data rate of the UTs in clear sky is shown. The use of DRA guarantees higher peak data rates over a larger number of user terminals if compared to a system using ACM only, and still allows for a good total offered capacity as from TABLE III. Therefore, the application of the combined ACM+DRA technique brings to a better trade/off between capacity and peak data rate.

V. CONCLUSIONS

In this paper, we analyzed two different approaches for IFMTs in a return channel of a multi-spot beam system based on DVB-RCS2. In addition to classical ACM technique, an algorithm for the joint usage of ACM and DRA has been considered. The target of the combined technique has been to equalize the PSD of the signals received at satellite level by adapting the symbol rate, while the capacity optimization is still performed with ACM. After defining the reference system scenario and assumptions, a set of performance results has been presented and compared to a system using just ACM. From the obtained simulation results, it is evident that the major advantage for combining DRA and ACM is represented by a larger distribution of high peak data rates to the UT population. The use of DRA brings also better results in terms of availability as the DRA range can be used to improve SNIR statistics under fading. Therefore, the conclusion of this work is that the adoption of a combined DRA and ACM technique can result in a better trade-off among all the key system QoS parameters, i.e. throughput, availability and user terminal peak data rates, if compared to classical ACM schemes. These considerations, are derived for a multi-spot system with very high number of beams, targeting terabit-satellite communications, but could as well apply to other networks where the intra-system interference plays and important role. Future works could consider a non-ideal scheduler and remove the assumptions of carrier segregation and organization among the beams, implying that a user can be interfered by any UT of the co-channel beams, regardless of their symbol rate. It is expected that such evaluation requires a more complex calculation of the interference statistics.

TABLE III. PERFORMANCE RESULTS SUMMARY

Figure of Merit	***ACM***	***ACM+DRA***	***Unit***
Average Total offered Capacity	133.5	134.8	Gbps
Average Spectral Efficiency	1.34	1.35	Bit/s/Hz
Spatial availability for 99.5% of time availability	35	86.5	%

a. The term “average” refers to an averaging both in space, i.e. over the coverage, and time, i.e. over the various fading events with the related probabilities

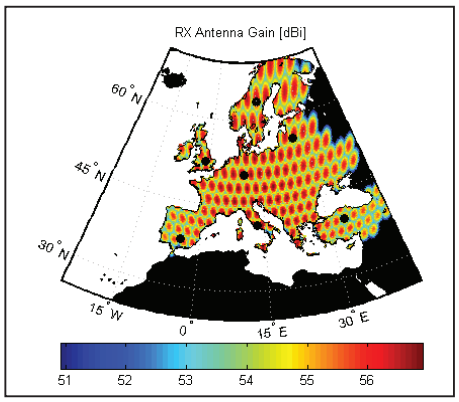

Figure 4 Satellite Antenna Coverage and RX gain; The location fo the gateway is indicated with a black circle

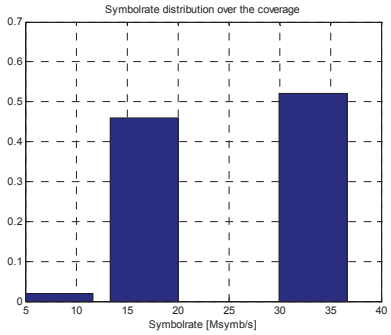

Figure 5 DRA symbol rate distribution over the coverage in clear sky

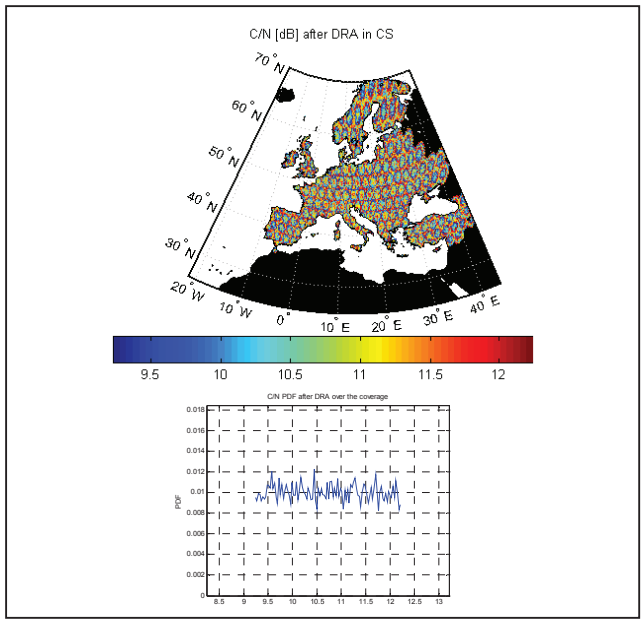

Figure 6 Up-link C/N distribution of ther coverage in clear sky

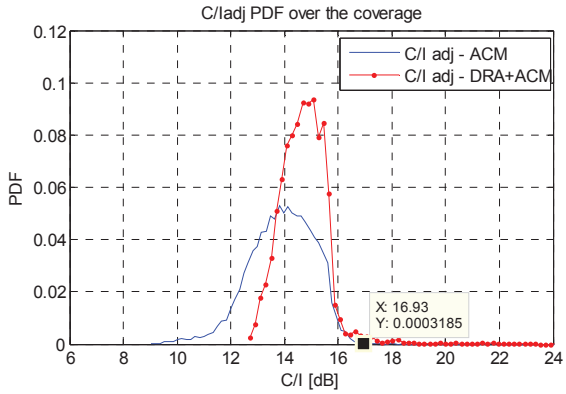

Figure 7 Comparison between the adjacent C/I in clear sky of a system using ACM and one using ACM+DRA

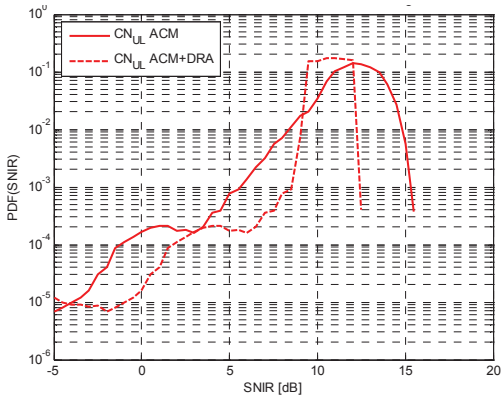

Figure 8 Time-averaged up-link C/N distribution over the coverage: comparison between ACM and ACM+DRA

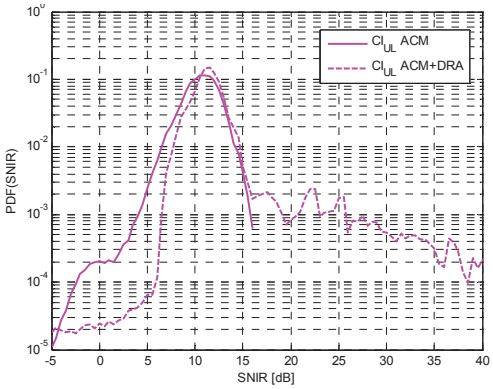

Figure 9 Time-averaged up-link C/I distribution over the coverage: comparison between ACM and ACM+DRA

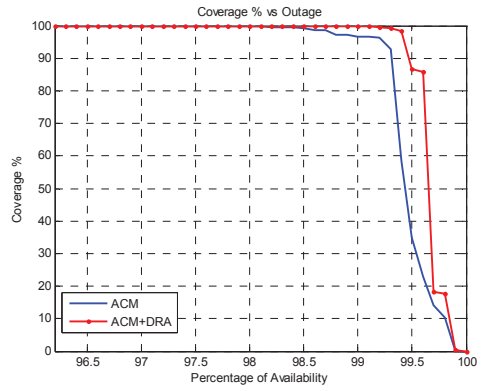

Figure 10 Percentage of coverage where the link is closed as a function of the end-to-end availability: comparison between ACM and ACM+DRA

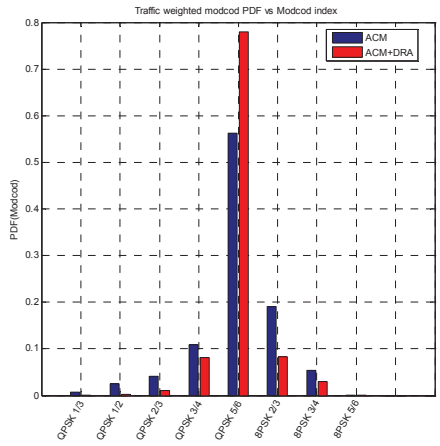

Figure 11 Average Modcod Distribution over the coverage: comparison between ACM and ACM+DRA

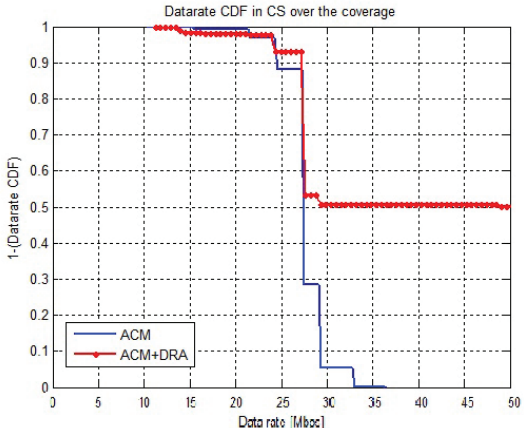

Figure 12 Peak Datarate Distribution over the coverage in clear sky: comparison between ACM and ACM+DRA

REFERENCES

[1] Digital Video Broadcasting (DVB); Second Generation DVB Interactive Satellite System (RCS2) Part 1: Overview and System Level specification. DVB Document A155-1 March 2011

[2] ETSI EN 301 545-2 V1.1.1 (2012-01) Digital Video Broadcasting (DVB); Second Generation DVB Interactive Satellite System (DVB-RCS2); Part 2: Lower Layers for Satellite standard

[3] ETSI EN 301 790 V1.5.1 (2009-05) European Standard Digital Video Broadcasting (DVB); Interaction channel for satellite distribution systems

[4] ETSI TR 101 790 V1.4.1 (2009-07) Technical Report Digital Video Broadcasting (DVB); Interaction channel for Satellite Distribution Systems; Guidelines for the use of EN 301 790

[5] R. Rinaldo, R. De Gaudenzi, "Capacity Analysis and System Optimization for the Reverse Link of Multi-beam Satellite Broadband Systems Exploiting Adaptive Coding and Modulation", submitted to Wiley Int. Journal on Satellite Communications, 2004

[6] S. Cioni, R. De Gaudenzi, and R. Rinaldo, "Adaptive coding and modulation for the reverse link of broadband satellite networks," in IEEE Global Telecommunications Conference,, vol. 2, Nov. 2004, pp. 1101–1105.

[7] "Dynamic Rate Adaptation (DRA) and Adaptive Coding and Modulation (ACM) efficiency comparison for a DVB-RCS system" Castro, M.A.V.; Ronga, L.S.; Werner, M.; Wireless Communication Systems, 2005. 2nd International Symposium on Digital Object Identifier

[8] R. De Gaudenzi, A. Ginesi and R. Rinaldo "Trade-offs Between Adaptive Conding and Modulation and Dynamic Rate Adaptation for the Reverse Link of Broadband Systems"

[9] Reccomendation ITU-R P.618-10 (10/2009) "Propagation data and prediction methods requred for the design of Earth-space telecommunication systems"methods requred for the design of Earth-space telecommunication systems"

[10] Cioni, R. De Gaudenzi and R. Rinaldo, "Channel estimation and physical layer adaptation techniques for satellite networks exploiting adaptive coding and modulation", Wiley Int. J. Satell. Commun. and Networking, Volume 26, Issue 2, March/April 2008 pp. 157-188. submitted.